

1 Article

2 **Tunnel configurations and seismic isolation optimization in**  
3 **underground gravitational wave detectors**

4 **Florian Amann<sup>1</sup>, Francesca Badaracco<sup>2,\*</sup>, Riccardo DeSalvo<sup>3</sup>, Luca Naticchioni<sup>4</sup>, Andrea Paoli<sup>5</sup>, Luca Paoli<sup>5</sup>, Paolo**  
5 **Ruggi<sup>5</sup>, Stefano Selleri<sup>6</sup>**

- 6 <sup>1</sup> Engineering Geology, RWTH Aachen, Lochnerstrasse 4-20 D-52064 Aachen, Germany; amann@lih.rwth-  
7 aachen.de  
8 <sup>2</sup> Centre for Cosmology, Particle Physics and Phenomenology, Université catholique de Louvain, Louvain-La-  
9 Neuve, B-1348, Belgium; francesca.badaracco@uclouvain.be  
10 <sup>3</sup> University of Utah, Dep.t of Physics & Astronomy, 115 South 1400 East 0830 Salt-Lake-City UT 84112 (USA)  
11 Università del Sannio, C.so Garibaldi 107, I 82100, Benevento (Italy),  
12 Riclab LLC, 1650 Casa Grande Street, Pasadena, CA 91104 (USA); riccardo.desalvo@gmail.com  
13 <sup>4</sup> INFN - Sezione di Roma, 00185 Roma (Italy); luca.naticchioni@roma1.infn.it  
14 <sup>5</sup> EGO, European Gravitational Observatory, Via Edoardo Amaldi, 556021 Cascina (PI. Italy);  
15 andrea.paoli@ego-gw.it, luca.paoli@ego-gw.it, ruggi@ego-gw.it  
16 <sup>6</sup> University of Florence, Dept. of Information Engineering; Via di S. Marta, 3, 50139 Firenze, (Italy)  
17 INFN Sezione di Firenze-Urbino, via G. Sansone, 1, 50019, Sesto Fiorentino (FI) (Italy); stefano.selleri@unifi.it  
18 \* Correspondence francesca.badaracco@uclouvain.be  
19

**Citation:** Lastname, F.; Lastname, F.;  
Lastname, F. Title. *Appl. Sci.* **2021**, *11*, 20  
x. <https://doi.org/10.3390/xxxxx>

Academic Editor: Firstname Last-  
name

Received: date

Accepted: date

Published: date

**Publisher's Note:** MDPI stays neu-  
tral with regard to jurisdictional  
claims in published maps and institu-  
tional affiliations.



**Copyright:** © 2021 by the authors. Sub-  
mitted for possible open access publica-  
tion under the terms and conditions of  
the Creative Commons Attribution (CC  
BY) license (<http://creativecommons.org/licenses/by/4.0/>).

**Abstract:** The Einstein telescope will be a Gravitational wave observatory comprising six nested detectors, three optimized to collect low frequency signals, and three for high frequency. It will be built a few hundred meters under Earth's surface to reduce direct seismic and Newtonian noise. A critical issue with the Einstein telescope design are the three corner stations, each hosting at least one sensitive component of all six detectors in the same hall. Maintenance, commissioning, and upgrade activities on a detector will cause interruptions of the operation of the other five, in some cases for years, thus greatly reducing the Einstein telescope observational duty cycle. This paper proposes a new topology that moves the recombination and input-output optics of the Michelson interferometers, the top stages of the seismic attenuation chains and noise inducing equipment in separate excavations far from the tunnels where the test masses reside. This separation takes advantage of the shielding properties of the rock mass to allow continuing detection with most detectors even during maintenance and upgrade of others. This configuration drastically improves the observatory's event detection efficiency. In addition, distributing the seismic attenuation chain components over multiple tunnel levels allows the use of effectively arbitrarily long seismic attenuation chains that relegate the seismic noise at frequencies farther from the present low-frequency noise budget, thus keeping the door open for future upgrades. Mechanical crowding around the test masses is eliminated allowing the use of smaller vacuum tanks and reduced cross section of excavations, which require less support measures.

**Keywords:** Gravitational waves, Einstein Telescope, Newtonian noise, observatory, seismic attenuation, tunnel configuration, observational efficiency

## 1. Introduction

Gravitational waves (GW) are detected by the relative motion that they induce between suspended test masses separated by large distances. To detect that motion, four test masses are configured as the mirrors that compose two long Fabry Perot interferometers that form the arms of a Michelson gravitational wave detector. The optical elements need

to be extremely well isolated from vibrations (i.e. seismic induced) that otherwise would overwhelm the gravitational wave-induced motion.

### 1.1. Why underground

The Einstein Telescope (ET) will be a European third-generation GW detector that will be built underground. It will be constituted by three nested GW interferometers in a triangular shape with sides of 10 km [1].

The ubiquitous seismic waves propagating with sub-micron amplitude through Earth's crust cause the so-called seismic noise, which is a mechanical movement that can be filtered away from a gravitational wave detector noise budget using sufficiently long and well-designed seismic attenuation chains [2]. Seismic waves also induce a much subtler effect that cannot be shielded. They cause tiny fluctuations of rock's density and position, which in turn generate tiny, local fluctuations of Earth's gravitational field that are seen by the detector as fluctuating space-time warps. This is called Newtonian noise [3]. Its effect on the test masses cannot be distinguished from the effect of a passing gravitational wave. The Newtonian noise acceleration depends linearly on the amplitude spectral density of the seismic displacement, which, at the frequencies of interest for ET, decays as  $1/f^2$ . Therefore, the Newtonian noise displacement amplitude spectral density will fall as  $1/f^6$  [4] affecting the sensitivity below 30 Hz and intervening in the noise budget only at low frequency.

Gravitational wave detectors that are built underground are substantially less influenced Newtonian noise. Yet Newtonian noise will eventually limit the sensitivity at low frequency of any Earth based detector. At the surface, air density fluctuations due to infrasound pressure waves and wind turbulence contribute to Newtonian noise [5]. The air density fluctuations in the atmosphere are not too relevant for underground detectors that are sufficiently deep [6].

The large density difference between soil and air, the low elastic constant of soil and the larger displacement amplitude of both surface and body waves that increase their amplitude when surfacing cause large Newtonian noise on test masses hanging near the surface. Surface waves dominate the surface Newtonian noise spectrum, but their amplitude diminishes exponentially with depth and frequency [3]. This means that their contribution to Newtonian noise decreases exponentially with depth. Body waves are present at all depths. Even if their amplitude diminishes with the higher stiffness of deep rock, their Newtonian noise remain present at all depths. The depth chosen for the Einstein telescope, about 300 m, was chosen as a tradeoff between diminishing returns and cost.

In theory, Newtonian noise could be estimated from a densely spaced network of seismometers surrounding the test masses and subtracted from the detector signal. This would require many high-precision seismometers optimally located in the rock surrounding the detector at distances comparable to the seismic wavelength generating the Newtonian noise, i.e. hundreds of meters. The method is further limited by the precision and the number of seismic sensors installed and by the mixing of shear and compressional waves that spoil the correlations between the inertial sensors used for the Newtonian noise estimation [7]. The quieter conditions inducing less Newtonian noise are the main rationale why future gravitational wave detectors aiming to detect gravitational waves down to 3 Hz [8] will be built underground. It will be shown that the proposed topology also allows almost optimal deployment of the inertial sensors required for an effective Newtonian noise subtraction.

All these improvements make ET a powerful and exciting instrument for gravitational wave astronomy.

An alternative approach, chosen for the Cosmic Explorer design [9], is to make a longer detector on the surface, diluting the fractional error of the larger surface noise with the larger amplitude of signals detected over longer distances. Subtraction of the much larger Newtonian noise present at the surface is possible but not sufficient to reach the desired low frequency sensitivity of the Einstein telescope. Underground locations are

99 always advantageous to detect the lowest frequencies needed to acquire the signals from  
100 heavier black holes. Barring unforeseen developments to mitigate Newtonian noise,  
101 gravitational waves at frequencies close to or less than 1 Hz can only be detected with  
102 space probes like LISA [10], DECIGO [11] or with Lunar gravitational wave antennas like  
103 LGWA , GLOC or LSGA [12-14].

### 104 1.2. The ET observatory detection efficiency

105 Gravitational waves happen all the time, their signals will even overlap in the Ein-  
106 stein telescope bandwidth. But interesting events like close-by neutron star inspirals or  
107 supernovae, that can give us detailed insight of astrophysics processes are rare [15]. The  
108 Einstein telescope must be able to continuously observe gravitational waves to avoid  
109 missing rare events. In principle it has sufficient redundancy (three nested detectors) for  
110 continuing observation even if a detector is out of service. This is a unique feature, but  
111 this redundancy is fragile. The catch is that in the present design each detector requires  
112 commissioning, upgrade and maintenance activities stretching over years. As a result,  
113 even single detector observatories like current Virgo and LIGO provide astronomical ob-  
114 servation only for a small fraction of the time. The observational efficiency will be even  
115 worse with six detectors needing attention or upgrades because, having at least one criti-  
116 cal element of all six detectors in each of the three corner stations, activity on a single  
117 detector will impede observation with all the other five.

118 We present a tunneling configuration that physically separates all critical compo-  
119 nents to increase the observatory's effectiveness and allow uninterrupted astronomical  
120 observations.

### 121 1.3. The xylophone concept and low frequency sensitivity

122 It is foreseen that the Einstein telescope triangle will host three pairs of interferome-  
123 ters [16]. Each pair will comprise a room-temperature detector specialized for higher fre-  
124 quency gravitational waves and a cryogenic detector optimized for low frequency signals.

125 The room-temperature, high-frequency detector will run with more than a megawatt  
126 of standing optical power to reduce the shot noise and increase the sensitivity at high  
127 frequency. The cryogenic, low-frequency detector will use only kilowatts of stored opti-  
128 cal power to minimize radiation pressure noise at low frequency and will require cryo-  
129 genic, long, and soft suspensions as well as crystalline test masses to reduce thermal noise.  
130 In the noise budget of the present Einstein telescope low frequency design, the residual  
131 seismic noise, suspension thermal noise, Newtonian noise and quantum noise contribute  
132 at a comparable level to the low frequency sensitivity limit. Suspension thermal noise  
133 can be pushed to lower frequency by longer, more flexible, and colder suspensions. Quan-  
134 tum noise can be mitigated by using heavier masses and quantum noise squeezing. Better  
135 sensors and technologies may be developed to subtract Newtonian noise. These im-  
136 provements may happen during the expected 50-year facility lifetime. It is therefore im-  
137 portant that the design of the seismic attenuators of the Einstein telescope facility will not  
138 impose a limit to the low frequency sensitivity, including for unforeseen future upgrades  
139 using techniques that are not yet anticipated.

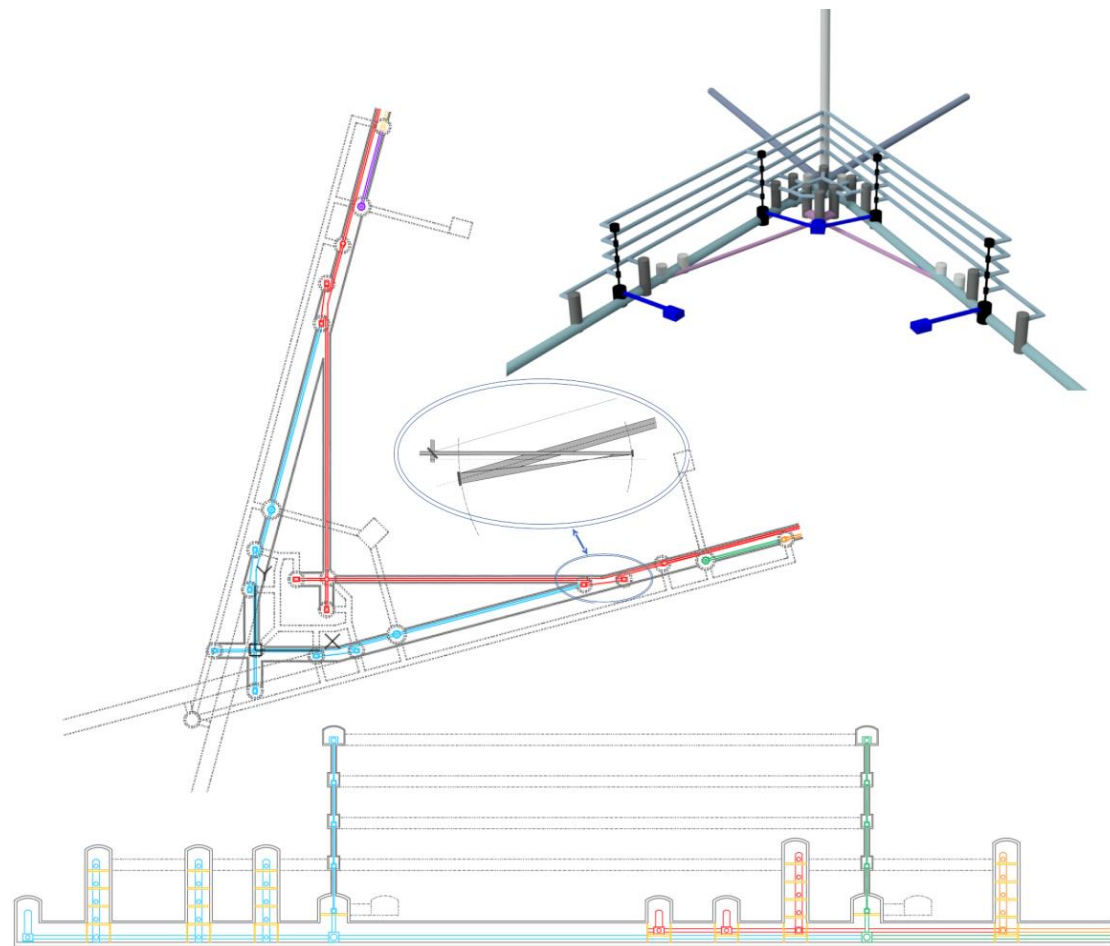
140 The long isolation chains that can be implemented in the proposed configuration can  
141 push the seismic noise of the Einstein telescope Low Frequency detectors well below the  
142 other limiting factors, keeping an open door for further upgrades. Perhaps more im-  
143 portantly, the long chains may ease some of the control noise issues. The proposed under-  
144 ground configuration also allows placement of inertial sensors in spherical patterns for  
145 optimal Newtonian noise subtraction.

## 146 2. Structure of present and future detectors

147 Terrestrial gravitational wave detectors are kilometer-scale Michelson interferome-  
148 ters with arms equipped with Fabry Perot cavities to extend their effective optical length.

149  
150  
151  
152  
153  
154  
155  
156  
157  
158  
159  
160  
161  
162  
163  
164  
165

The Fabry-Perot mirrors are heavy test masses suspended from threads, so that they can be freely accelerated along the beamline by the space-time fluctuations caused by passing gravitational waves. Present surface detectors (Virgo, LIGO, KAGRA [17-19]) have arms 3 to 4 km long, while future detectors currently being designed will be three to ten times longer. In the current surface L-shaped detectors, input test masses, recombination and input-output optics are housed in a single large building. The present design of the Einstein telescope has three 10 km long tunnels oriented at 120° from each other. The six nested detectors are intended to record signals from both polarizations of gravitational waves. They intersect in three large vertex halls, each containing eight of the twenty-four test masses, including at least one of all six detectors, as well as the input/output optics of two Michelson interferometers and their ancillary equipment. This configuration has several drawbacks including excessive crowding and mixing of optical components and seismic isolation systems, that require quiet conditions, with ancillary equipment, such as cryogenic chillers that cause reverberating acoustic noise, which is known to inject noise into the interferometer. The worst concern is that access for maintenance or upgrade on a single detector will affect, and in most cases impede, the operation of all others, thus reducing or interrupting astronomical observations every time that an access is made.



166  
167  
168  
169  
170  
171  
172  
173  
174

**Figure 1:** Top left: Configuration for separate extraction of the two interferometers from the main tunnel and a possible structure for access tunnels. The insert is a zoom onto the beam-reducing telescopes that extract the Michelson beams from the main tunnel. The room temperature interferometer, which is located above the cold one, (red) is extracted first, thus leaving more space for the cryostats of the low frequency detector (blue). Input and output optics (not detailed here) are housed together with the beam splitter in separate L-shaped excavations of reduced volume. Bottom: Elevation view of vertical structures with different kinds of seismic attenuation chains. All access tunnels (behind or in front of the tunnel vertical section) are represented with dotted

175 lines. The 3D insert on the top right corner is a sketch provided to guide the eye, an interactive 3D  
176 version is provided in figure 9 of the online-only appendix.

### 177 2.1 *Underground stability constraints*

178 The Einstein telescope will be built at about three hundred meters below the surface.  
179 Strong and massive, moderately jointed (i.e., unfractured or slightly fractures) rock mass  
180 conditions, dry or with a low hydraulic conductivity are assumed. Underground con-  
181 struction causes a stress redistribution around the excavation that may exceed the rock  
182 strength or cause rock creep [20]. In tunnel designs with many adjacent large excavations,  
183 the redistributed stresses of individual excavations will superimpose and intensify. It is  
184 therefore important to allow for rock walls wider than the excavated volumes between  
185 large voids, such as at the intersection of the halls at the corner points to avoid failures  
186 started by blast damage or superimposed stress states.

187 The proposed design, sketched in Figure 1, is only indicative, the lengths and exca-  
188 vation shapes must be optimized to satisfy science requirements and avoid all structural  
189 weakness. Large excavations often suffer from structural controlled instabilities, e.g.  
190 rock wedges, that are formed by intersecting discontinuities such as joints or small fault  
191 planes, which require heavy rock support, e.g. long and heavy rock bolts or anchors, thick  
192 reinforced concrete lining, and more. The stability issues at the target depth of the Einstein  
193 telescope are mostly relevant for the large caverns in the corner points, where the size of  
194 the excavation damage zone or structural controlled rock wedges could also be large. The  
195 instability is fully mitigated by the reduced size and rounded shapes, i.e. curved side walls  
196 instead of vertical side walls. Detailed size and shape adjustments can be done in an early  
197 design stage by optimizing the distribution of the detector components and their mode of  
198 access through the rock mass once the rock mass conditions are known through a site  
199 investigation program.

### 200 2.2 *Other underground constraints*

201 In addition to stability considerations, the corner stations host access tunnels or shafts  
202 with constraints that need to be considered. The ET facility is expected to last 50 years.  
203 The LIGO Livingston observatory experience teaches that in an environment with high  
204 humidity after only 20 years corrosion can degrade the vacuum works and cause leaks  
205 even in pipes built with stainless steel. Underground water and airborne agents are usu-  
206 ally more aggressive than at the surface. Water ingress must therefore be avoided either  
207 by an optimal positioning of the facility in dry rock with low permeability or by systematic  
208 grouting, sealant injections and surface lining to reduce the rock mass hydraulic conduc-  
209 tivity and eliminate accumulating or steady-state inflow rates. Any water must be im-  
210 mediately collected through a drainage pipe system and routed out. Available data in-  
211 dicates that the Sos Enattos site is likely to satisfy this important requirement. The local  
212 mine drainage flow is of the order of one liter per second from its ~ 50 km of galleries and  
213 the electrical resistivity tomography of the site shows the absence of significant ground-  
214 water, due to the low porosity of the rock [21].

### 215 2.3 *The proposed tunnel configuration*

216 The tunnel configuration sketched in figure 1 takes best advantage from the under-  
217 ground environment for building gravitational wave observatories. It consists in several  
218 small and interconnected stable excavations. Angled, beam-reducing telescopes posi-  
219 tioned upstream of the input test masses produce extracted beams that propagate at a 15o  
220 angle away from the Fabry Perot direction, so that the recombination on the beam splitter  
221 happens at the optimal 90°. A suitable separation along the tunnel of the input test masses  
222 of the two Michelson interferometers causes the extracted beams to cross in separate ex-  
223 cavations that house the beam-splitter and input/output optics [22].

224 The fundamental limitations of low-frequency sensitivity of gravitational waves, i.e.  
225 quantum noise, radiation pressure, and suspension thermal noise are not addressed here.

We only note that mitigation of suspension thermal noise requires substantial vertical space above the test masses, which is made available by this configuration. The proposed scheme is also suitable for upgrades to heavier masses to reduce the quantum back-action noise.

#### 2.4 Present Seismic Attenuation Systems

Seismic noise attenuation comes from the natural properties of a pendulum, which attenuates horizontal vibration transmission with a  $1/(f^2-f_0^2)$  function that provides a cutoff starting above the pendulum resonant frequency  $f_0=\sqrt{gl}/(2\pi)$  where  $l$  is the pendulum length and  $g$  is the gravitational acceleration. The mechanical attenuation is provided by a chain of pendulum wires alternated to massive vertical attenuation filters (discussed in Section 3.3) acting as pendulum mass. Each stage contributes a  $1/(f^2-f_0^2)$  attenuation starting from its corresponding resonant frequency. With  $n$  stages a  $1/(f^2-f_0^2)^n$  attenuation power is achieved [25]. Therefore, seismic attenuation performance on the low frequency side is limited by the length of the pendulums used, which are limited by the height available above the test masses.

The overall length of the seismic attenuation chains of present detectors ranges from a couple of meters in LIGO [17], to seven meters, in Virgo [18]. Most present detectors (except for KAGRA) rely on support structures extending up from the tunnel floor encroaching in the volume around the test masses. Tall structures need to be very stiff to avoid amplifying ground motion and their height is limited by the hall that hosts them. Individual pendulums in present detectors are limited to lengths of the order of a meter, with resonant frequencies (start of passive attenuation) distributed around 0.5 Hz. This is adequate for a detection threshold above 10 Hz but not for the lower detection frequency of the Einstein telescope.

#### 2.5 Present design of Einstein telescope Seismic Attenuation System

The Einstein telescope aims to be sensitive below 10 Hz, thus requiring the start of the  $1/(f^2-f_0^2)$  roll offs at lower frequencies than present detectors, and therefore longer pendulums. The attenuation chain length in the current Einstein telescope design is limited by the foreseen excavation ceiling height to 17 m tall towers [8]. Each tower contains six stages of pendulums with less than 3 m long suspension wires. The resonant frequencies of 3 m long pendula are close to 0.3 Hz (0.49 Hz in Virgo 1 m pendula). With these limitations in vertical size, seismic noise remains a small but non-negligible source of noise at the lowest frequencies, which may become a limiting factor if new ways are found to further depress quantum, suspension thermal and Newtonian noise.

#### 2.6 The proposed seismic attenuation structures

The two taller structures in the lower panel of figure 1 are stacks of excavations (alcoves) connected by a vertical borehole. Each alcove harbors one of the vertical attenuation filters separated by pendulums longer than 10 m. They provide isolation for the most demanding cryogenic test masses of the low frequency interferometers. The dotted side excavations near the base of these stack (dark blue in the 3-D insert) house the noisy cryogenic chillers. Separate excavations are needed to isolate the vibration noise caused by the more than 150 kW of cryo-chiller power needed to cool the test masses and long vibration-isolated cryogenic shroud and baffles. These baffles extend for more than 50 m and have two requirements. They are needed to intercept all possible trajectories of water molecules that may otherwise reach and deposit on the mirror surfaces and must be vibration isolated to neutralize the effects of residual scattered light. The cooling power is delivered at an appropriate height along the seismic attenuation chains, with an appropriate separation from the test masses.

274 Any other noisy equipment can be housed in similar alcoves. The access tunnels can  
275 be configured to reroute most of the main tunnel ventilation away from the test masses  
276 and recombination optics, where turbulence may cause atmospheric Newtonian and  
277 acoustic noise.

278 The five intermediate-length towers, also shown in figure 1, are for the room-temper-  
279 ature interferometer test masses and other main optical elements. They may be of differ-  
280 ent kinds and heights, depending on specific requirements. The three smallest structures  
281 contain seismic isolation for optical benches and other less demanding optics. An im-  
282 portant point is that all seismic attenuation chains can be anchored to the rock above to  
283 avoid encroachment of support structures around the optical elements. The inverted pen-  
284 dulum and top filter at the head of the long chains sit directly on the rock floor in the top  
285 alcove.

286 It is important to note that alcoves with narrow and sealable access tunnels proved  
287 very effective to isolate from ambient noise or vibrations induced by ventilation or other  
288 machinery. When installing seismometers in the Homestake mine [23] it was observed  
289 that the instruments installed in similar alcoves had the lowest noise floor.

290 The elimination of structural encroachment around the test masses is especially val-  
291 uable in the locations where the beams of the high frequency interferometer peel off from  
292 the main tunnel and to make space for the cryostats. The test masses can be simply  
293 housed along the main tunnels with little or no local tunnel enlargement.

294 Other advantages provided by the proposed configuration are detailed in the follow-  
295 ing sections.

296 We stress that the sketch of figure 1 is only conceptual, reasonable dimensions are  
297 suggested but not optimized. Exact topology, height, load, or size of attenuation stages  
298 for different optical elements are not yet determined. The vibration isolation solutions  
299 outlined can be scaled to meet the different requirements of various optical elements while  
300 easy access to all attenuation chain elements can be maintained. Similarly, no effort is  
301 made here to decide excavation shapes and sizes, or to decide spacing along the beams to  
302 eliminate interference between different detectors. This will be object of a complex  
303 tradeoff study involving mining engineers and physicists, with the aim to minimize costs,  
304 maintain safety and satisfy all scientific requirements. A rough cost comparison between  
305 the ET baseline design and the one proposed here was made [24]. The larger excavation  
306 volume of the first balance the greater complexity of the second. Within the evaluation  
307 error margin, no significant cost difference was found.

### 309 3. Advantages of the proposed configuration

#### 310 3.1 *Segregating the critical components of different detectors in separate caverns.*

311 Decoupling the maintenance, upgrades and/or commissioning of different detectors  
312 in the Einstein telescope is of crucial importance because, it allows to work on one detector  
313 without affecting the operation of the others and to maintain continuous observation  
314 mode.

315 The separation of the recombination and input-output optics of different detectors in  
316 individual excavations and their separation from the test masses is discussed in [22] and  
317 illustrated in figure 1. The key point is that just a few meters of rock provide much more  
318 isolation of what exists between the interferometers and their control rooms in present  
319 surface detectors. Similarly, access to the main tunnels housing the test masses may not  
320 affect the operations because the support points of the seismic attenuation chains from  
321 which vibrations may be injected reside on hard rock at higher tunnel levels and therefore  
322 are insensitive to activity in the main tunnel. Working on a detector can be expected to  
323 not affect the operation of the other five.

#### 324 3.2 *Low Frequency Seismic noise and reduction of out-of-band r.m.s. motion.*

325 There are serious concerns about the interferometer control noise. Forces are needed  
326 to maintain the lock of the interferometer with sufficient authority to compensate for the  
327 residual motion of the suspension chains below the gravitational wave detection band.  
328 These out-of-band control forces can generate up-conversion and inject control noise in  
329 the detection band [26]. There is substantial advantage in lowering the isolation system  
330 resonant frequencies and in reducing the amplitude of the pendula residual motion. The  
331 longer oscillation periods of a longer pendulum allow more time for a force to act. Smaller  
332 control forces are required to control smaller amplitude motion. In both cases less control  
333 forces are required, and this results in less control noise.

### 334 3.3 *The attenuation chains as seismic sensors.*

335 Sensing the changing distance of the seismic attenuation filters with respect to the  
336 surrounding rock at various heights along the attenuation chains provides a measurement  
337 of the linear and tilt movements for active damping of the pendulum modes. It is also  
338 important to reduce the movements induced on the test masses by the micro-seismic peak  
339 [27,28]. In this regard, it should be noted that after acquisition of Fabry-Perot lock each  
340 pair of test masses effectively form a single, rigid inertial mass hanging from two widely  
341 separated points subjected to the seismic noise of two vertices of the triangle. After the  
342 Michelson lock acquisition, the four test masses of each interferometer form an even larger  
343 composite inertial mass with suspension points distributed in all three facility vertices.  
344 Optical levers, augmented with fringe counting, provide length sensing between each test  
345 mass and the surrounding rock. In the Einstein telescope triangular topology, the six  
346 locked detectors provide multiple independent measurements of the low frequency seismic  
347 motion with two different suspension frequency tunings and three orientations. These  
348 redundant signals can be combined to form synthetic seismometer measurements of the  
349 low frequency seism at the three vertices with noise floor substantially below what can be  
350 achieved with conventional sensors. These signals can be used to suppress the amplitude  
351 of low frequency motion caused by micro-seismic noise. All of this contributes to reduce  
352 the residual motion of the test masses and ultimately control noise.

### 353 3.4 *Multiple tunnel layers for lower-frequency seismic noise suppression*

354 The multiple level topology provides effectively unlimited vertical space and pendu-  
355 lum lengths. The start of the  $1/f^2$  roll off at lower frequency shifts the seismic noise farther  
356 from the Einstein telescope detection frequency band. Consider, for example, filters  
357 housed in 4 m tall excavations vertically separated by 8 m of rock. The resulting  $\sim 12$  m  
358 separation between filters is four times that in the current Einstein telescope design and  
359 produces pendulum resonances below 0.15 Hz. This arrangement, assuming the same  
360 number of filters, would cut in half the starting frequency of the seismic attenuation roll  
361 off. This of course works only if that frequency can be matched by vertical attenuation  
362 filters [28, 29] also tuned at or below 0.15 Hz (see chapter 5 for detail).

363 The attenuation performance of a 60 m long chain is compared in figure 2 with that  
364 of the 17 m chain of the Einstein telescope baseline design. The expected start of the at-  
365 tenuation curve at half the frequency is visible in the simulation at  $\sim 0.55$  Hz. The struc-  
366 ture above 0.55 Hz is contributed by suspensions that are not yet re-optimized. The dis-  
367 placement noise is compared in figure 3 by folding the attenuation transfer function of  
368 figure 2 with a typical underground seismic spectral noise (Data from [30]). Additional  
369 simulations show that with longer suspensions, made also possible by the proposed to-  
370 pology, the full gain from the longer wires can be recovered.

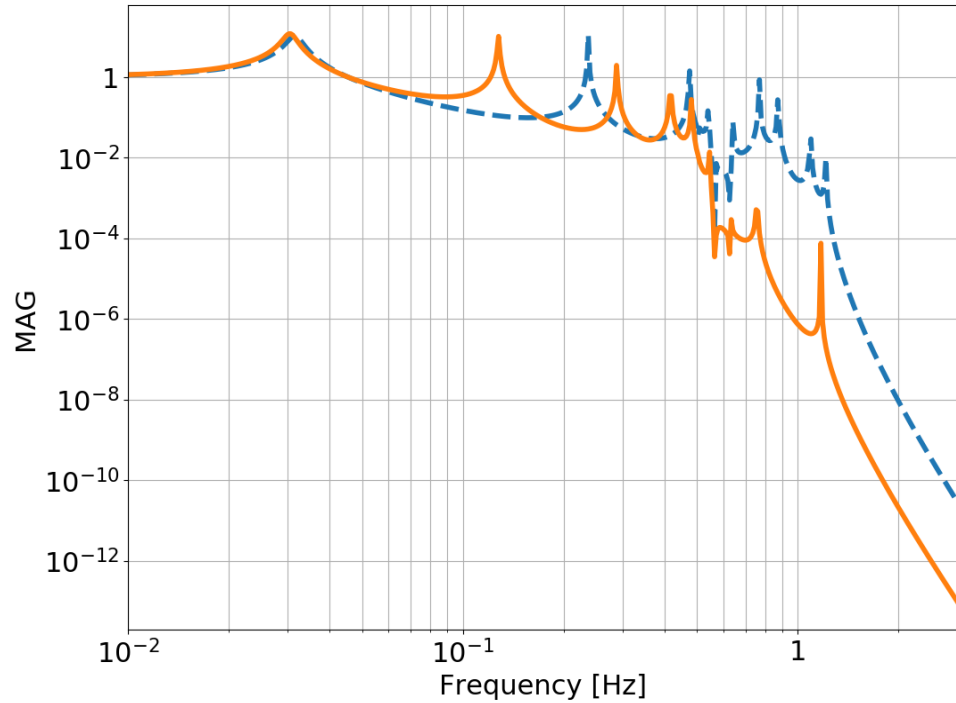
### 371 3.5 *Separating the top of the seismic isolation chain from the test mass level*

372 The scheme for seismic attenuation illustrated in figure 1 envisions vertical stacking  
373 of small excavations connected with boreholes for the pendulum wires. The only con-  
374 nections to ground are through the pre-isolators, which are relegated to the top level, and



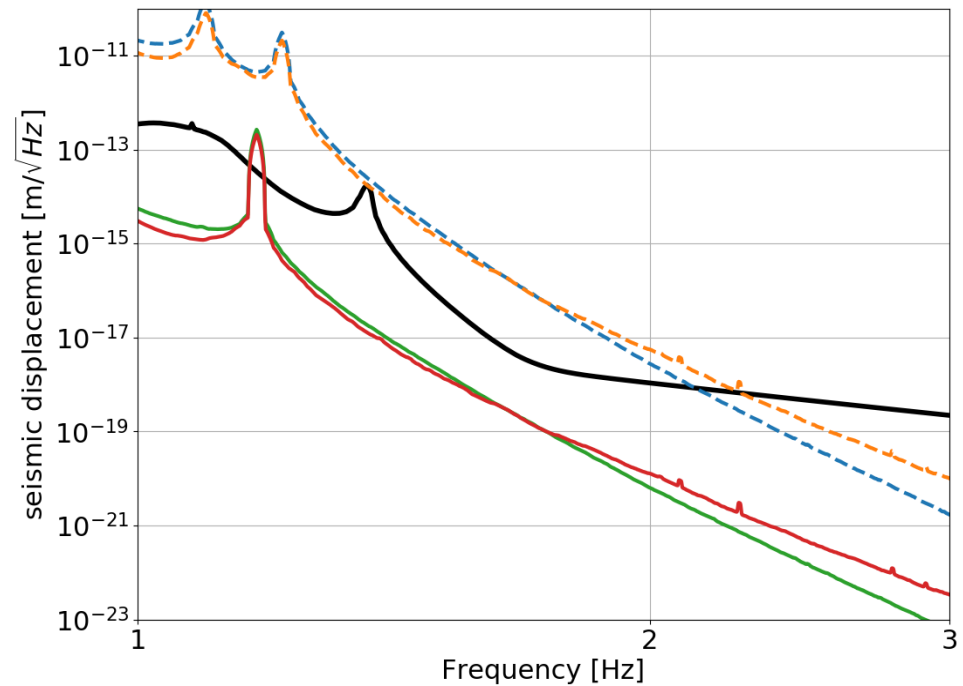
375  
376  
377  
378

through the cryogenic heat links [31]. The cryogenic heat links can be positioned at a suitable intermediate level of the attenuation chain to screen the test masses from residual mechanical noise from the chillers.



379  
380  
381  
382  
383

**Figure 2:** Comparison between the Einstein telescope baseline seismic attenuation scheme with 3 m separation between filters (orange, solid) and the same configuration with 12 m (blue, dashed) of separation between filters. The mirror suspensions are the same in the two simulations, without re-optimization for lower frequency performance.



384  
385  
386  
387

**Figure 3:** Comparison of the expected displacement noise after convoluting the transfer function with the measured seismic noise in Sos Enattos (blue and green) and Terziet (orange and red). The seismic data are taken to be the square root of the squared sum of the 90th percentile of the north

and the east channels. The dashed lines refer to the 17 m suspensions and the solid lines to the 60 m suspensions. The optical length sensing is expected to have a sensitivity around 10-18m/ $\sqrt{\text{Hz}}$  in this frequency range. The black line is the current design sensitivity curve of the Einstein telescope.

### 3.6 Smaller vacuum chambers

In Virgo and LIGO, the seismic isolation systems had to be contained and supported from the ground by bulky vacuum chambers requiring human access for installation and maintenance.

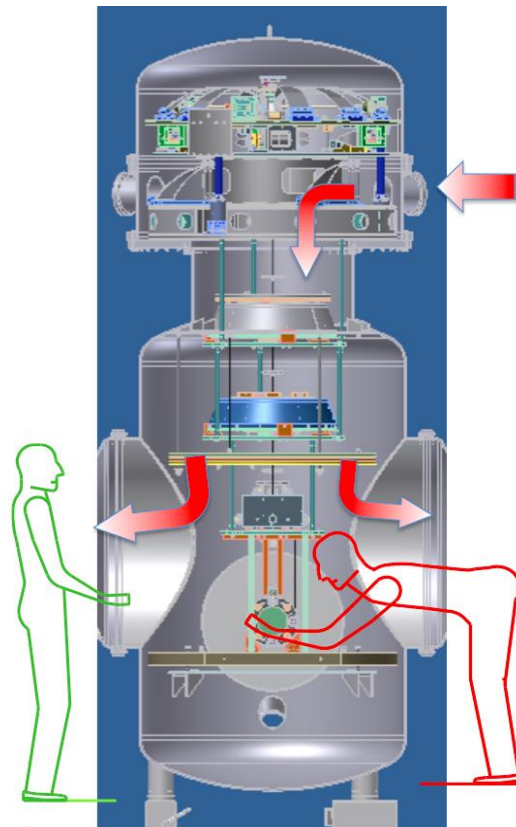


**Figure 4:** Ergonomic access to large optics in a reduced-size, side-access vacuum tank. The operators remain outside the vacuum chamber, thus reducing chances of introducing pollutants. The red arrows indicate a clean air flow. Having removed the encumbrances from the seismic attenuation structure, the same scheme can be applied to larger size optics, including cryostats equipped with removable lateral thermal shield panels, like those implemented in the CLIO and KAGRA cryostats.

Having relocated the seismic attenuation away from the main tunnel level, much smaller vacuum chambers can be used, including for the test masses. Similarly, moving the cryogenics in separate excavations, and injecting the heat links higher up in the attenuation chain allows the use of smaller gauge tunnels. While the larger payload integration in the Einstein telescope may still require access from below, as in Virgo, other operations of maintenance and tuning of the system may be possible from side access. Much cleaner working conditions than for the test masses of the present detectors can be obtained if the operator can work from the side of the vacuum chamber while the optics are continuously protected by a flow of clean air provided from above. This kind of side access has been successfully used in Japan since the TAMA detector [32]. The scheme illustrated in figure

4 was designed for beam size reducing telescopes in KAGRA [33] that use recycled, large initial LIGO test masses. The same side access configuration can be adapted for the larger and cryogenic optics of the Einstein telescope.

### 3.7 Access to suspension elements of the cold and warm interferometers

Access to upper elements of a seismic attenuation chain has always been a laborious enterprise, requiring removal of the vacuum chambers and involving tall and complex support structures that extend along the full chain's height. These structures recur in the wide excavations proposed for the Einstein telescope and occupy a significant fraction of the hall volume. Installation and upgrades pose significant technical challenges and risks.

In the configuration proposed here, side-access vacuum chambers in vertically separated alcoves provide easy and safe access for installation, tuning and upgrades of the long seismic attenuation chains.

### 3.8 Shorter seismic isolation chains

Seismic isolation for less demanding and auxiliary optics can be satisfied with more compact chains like those used for the main mirrors in KAGRA, as illustrated in appendix figure 8-left. An example of the complex mechanical structures required to mitigate the amplification of ground tilt on raised structures is illustrated in appendix, figure 8-right. This complexity and space encumbrance can be avoided even for short chains by attaching the top stage of their seismic attenuation chain to the rock above. The shorter chains leave no place for rock separated alcoves, rock-anchored platforms in wells will fulfill the same function of alcoves to provide easy access.

### 3.9 Segregating noisy equipment.

The cryogenic chillers for the 12 cryogenic test masses require a power of the order of 150 kW [34]. Chillers are notoriously noisy, especially at low frequency. To isolate the vibrations that they generate, it is necessary to house them in separate excavations, with anchoring to rock designed to filter out compressor vibrations and heat links running through boreholes. Several meters of rock efficiently shield the vibrations while the machinery can remain continuously accessible for maintenance via separate tunnels. It should be noted that the longer lengths involved may require replacing the external metallic heat links with liquid helium lines, which further reduce transmission of vibrations.

It is worth mentioning that water cooling will be necessary to evacuate the power consumed by the chillers, as well as for any other instruments requiring significant power. Air cooling cannot be relied on because fast air flows through the tunnels produce unacceptable levels of induced noise, including Newtonian noise.

## 4. High Frequency detectors and shorter chains

The Einstein telescope High Frequency detectors [16] feature less demanding attenuation chains with shorter pendulums. The stacked alcove configuration becomes unnecessary. These attenuation chain components can reside in rise-bore shafts extending above the main beam tunnel. The pre-isolator would rest on short beams anchored to the rock. The number, separation and size of filters needed would depend on the requirement of each specific optical element. Cylindrical vacuum chambers with side access flanges and balconies, all supported on the rock, provide ergonomic access to the chain elements for maintenance and tuning.

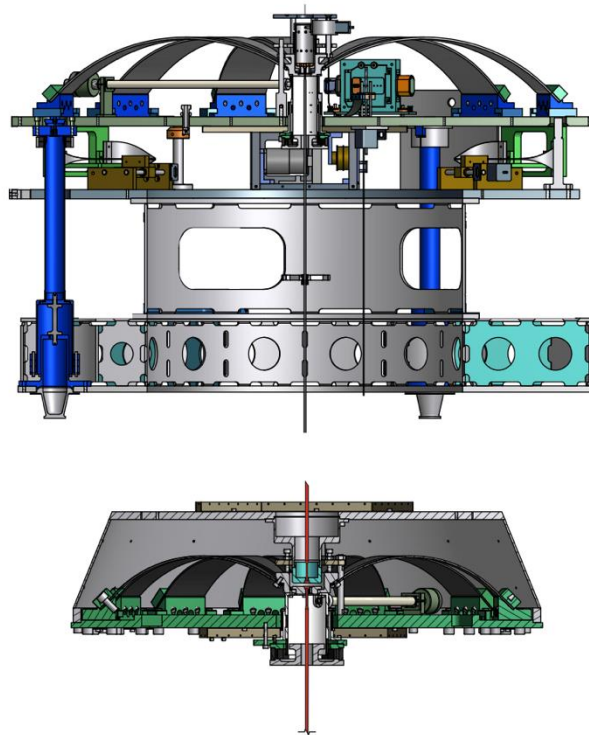
## 5. More on seismic attenuation

### 5.1. Vertical attenuation filters

The attenuation performance in the horizontal plane is spoiled if not accompanied, at every stage, by matching vertical attenuation. Because of unavoidable mechanical

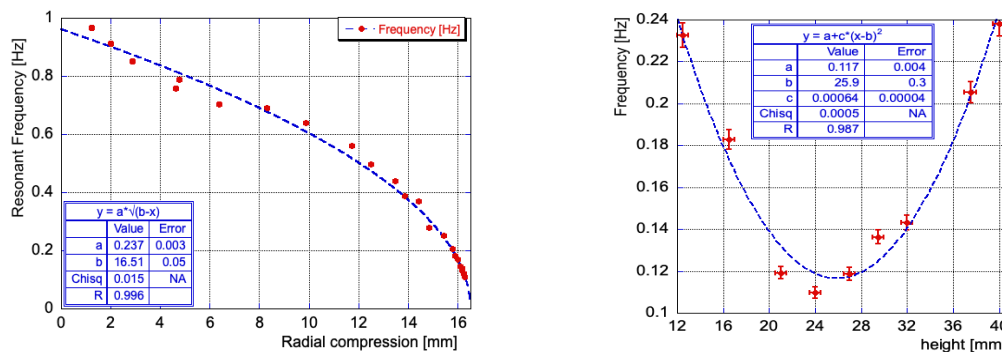
463  
464  
465  
466  
467  
468  
469  
470  
471  
472  
473  
474

imperfections and of the effects of Earth’s sphericity, vertical noise leaks into the horizontal plane at each step of an attenuation chain [2]. Suitable vertical attenuation can be achieved using modular Geometric Anti Spring filters in appropriate number and size to match the requirement of each individual optical element. The Geometric Anti Spring filter is a mature technology used in Virgo upgrades [35], HAM-SAS [36], TAMA [37], KAGRA and scientific and commercial platforms. They are sophisticated but simple mechanical oscillators that can be tuned to low resonances but were never required to operate at or above 0.15 Hz. Examples of two kinds of filters that can be re-sized to satisfy all the Einstein telescope requirements are illustrated in figure 5. The low frequency operation (0.12 Hz) shown in figure 6 was achieved for the top Geometric Anti Spring filters of KAGRA. This tuning already matches the resonant frequency of the longest pendula envisaged in this paper.



475  
476  
477  
478  
479  
480

**Figure 5:** A pre-isolator (top) and of a standard filter (bottom) designed and built for KAGRA. The pre-isolator is composed by a short, inverted pendulum footed directly on the bedrock in an alcove at the top. It supports a large Geometric Anti Spring filter that in its turn suspends a chain of standard filters. The standard filter is similar but smaller. Both can be scaled to the heavier payloads of the Einstein telescope.



481  
482  
483

**Figure 6:** Tuning of a KAGRA pre-isolator Geometric Anti Spring filter. Left: Frequency tuning of the resonant frequency obtained by radial compression of the cantilever blades forming the Geo-

metric Anti Spring mechanism [38]. Right: Dependence of the resonant frequency from the working point. The working point can be fine-tuned in situ via controls of the temperature of the vacuum tank.

A caveat is that low resonant frequency is achievable only over a very narrow dynamical range, as evident in the right panel of figure 6. If the resonant frequency is tuned to lower values, the frequency vs. height curve becomes progressively narrower. This tuning requires matching the spring strength to the payload weight at  $<10^{-4}$  level, which can be achieved with thermal control of individual filters. The Young modulus of steel changes by  $\sim 3 \cdot 10^{-4}/K$  with temperature. The required load matching can be achieved with a thermal control of a tenth of a degree, which is easily achievable in a vacuum tank. A range of several degrees is needed while up to 100 K of heating is allowable without inducing creep on properly treated maraging springs [39].

### 5.2. Pre-isolator short legs

A pre-isolation filter is foreseen at the top of each optical chain. It is composed by a short, inverted pendulum supporting a Geometric Anti Spring filter. Short inverted-pendulums have the same attenuation power of longer ones without being affected by the low-frequency internal resonances (banana modes) of longer legs. Long legs may weigh more than 100 kg while short ones supporting the same load weigh less than a kg. Therefore, their batting center and the recoil of their internal modes affects much less the heavy top filter. The counterweights for batting center compensation are less critical, and in some cases unnecessary [40]. By sitting directly on hard rock, the pre-isolators don't suffer from the amplification of ground tilt affecting tall structures [41,42], this is an invaluable advantage. The simple coupling of an inverted pendulum and a Geometric Anti Spring filter [43,44] provides a passive attenuation power equivalent to that of the entire Advanced LIGO active isolation without its control complexity [45]. While fundamentally a passive element, the inverted pendulum and top filter combination is also an ideal platform for active reduction of low frequency seismic noise with inertial sensor signals [46,47] or to apply feed-forward from other signals [48,49].

### 5.3. Test mass suspensions

The test masses in present, and future room temperature detectors, are suspended using fibers made of fused Silica [50]. This is also the solution chosen for the high frequency detector of Einstein telescope. Silicon, Sapphire, or other crystal rods will be needed to suspend and cool test masses in low-frequency cryogenic detectors [51,52]. In the Einstein telescope the suspensions will need to be longer and softer than in present detectors to reduce the suspension thermal noise that dominates at low frequency; yet they must have sufficient thermal conductivity to keep the mirrors at cryogenic temperatures. The design of the mirror suspension solutions with large compliance and thermal conductivity are considered elsewhere [53]. The proposed configuration provides the vertical height needed for suspension thermal noise mitigation.

## 6. Flexibility gains and limitations

The large halls in the present Einstein telescope design are intended to provide flexibility for future improvements of the facility. It has been argued that positioning seismic attenuation chains in wells would impede length tuning or reconfiguration of the optical cavities. While it is true that large changes of the Fabry Perot lengths will not be possible without re-shaping boreholes and excavations, there is little reason to do it and small length changes for tuning purposes remain possible within the diameter of the connecting boreholes. It should be considered that the input/output optics located in individual recombination halls will be easier to reconfigure because there is no interference with other detectors.

## 7. Radial boreholes and Newtonian noise subtraction sensors

534 Effective Newtonian noise subtraction techniques require numerous high-sensitivity  
535 sensors to instrument the rock mass surrounding the test masses. These sensors must be  
536 distributed in a pattern with a size comparable with the wavelength of the seismic waves  
537 of interest. At 2 Hz, with a seismic speed of 5 kilometer per second, the characteristic  
538 dimension is of the order of a kilometer. This is a large and expensive endeavor involv-  
539 ing tens of kilometers of borehole that may be justified only when the detector has reached  
540 sufficient sensitivity at low frequency. Experience shows that it takes years to build a  
541 gravitational wave detector and even more to reach the stage when Newtonian noise may  
542 become a limitation. It is thus necessary that the Newtonian noise mitigation can be  
543 staged and/or implemented at a later time, when better understanding of the require-  
544 ments is gained.

545 The required Newtonian noise cancellation system can be achieved with maximized  
546 effectiveness, minimized borehole length, and cost by directional drilling of boreholes ra-  
547 diating from tunnels located near the three corners. Directional boring techniques devel-  
548 oped for oil extraction and ore exploration [54] allow an optimal and easily expandable  
549 sensor geometry. Boreholes radiating from near the corner stations are sketched (in a  
550 plane) in figure 7. This geometry minimizes the drilling length and allows centralized  
551 signal collection. Implementation will require custom triaxial inertial sensors with remote  
552 anchoring/release and alignment mechanisms. Boreholes hundreds of meters in length  
553 can be drilled from one or two dedicated tunnels to instrument the volume surrounding  
554 the corner stations. Each borehole will host many sensors spread out at suitable distances  
555 to satisfy the optimal sensor distribution requirements.

556 The mono-axial sensing heads inside modern low frequency seismometers are small  
557 and require only small changes to fit within standard diameter boreholes, i.e. 130-170mm  
558 but precision self-alignment capability will be necessary. The installation must be per-  
559 formed remotely by crawlers capable to install and align or retrieve the sensors. An in-  
560 stallation procedure might be as follows. A mono-axial sensor is brought in place by a  
561 cable-controlled crawler. The sensor's outer housing is equipped with spring-loaded ex-  
562 pansion brakes for rigid connection to the borehole walls while a spherical bushing allows  
563 smooth rotation of the sensor head. Both the brakes and the bushing are of the normally  
564 locked type. They are released as needed with compressed air provided by the crawler.  
565 After positioning, the crawler locks the brakes to the walls, orients the sensor to level and  
566 align it, then locks the rotation. Finally, the crawler returns to fetch the next sensor that  
567 is connected to the previous one before starting its alignment procedure. The sensors are  
568 daisy chained along the borehole and installed in groups of three to get three-axial sensing  
569 while the spacing between the triplets is determined by the sensing requirements.

570 Boring produces vibrations. The tunnels hosting the drilling equipment must be at  
571 a distance, to be determined experimentally, from the detectors that the seismic attenua-  
572 tion chain can neutralize them.

573 Drilling vibration may still affect the length sensing of the interferometers through  
574 other channels like scattered light, possible up-conversions of control signals, and even  
575 Newtonian noise. The radiated vibration can be monitored with geophones placed near  
576 the source. Drilling can be regarded as a "known" point-like source of seismic noise. If  
577 any effect on sensitivity is observed during drilling operations, modern signal correlation  
578 techniques may identify, quantify, and possibly localize channels of length sensing noise  
579 injection. Drilling may therefore be an effective diagnostic tool to identify and eliminate,  
580 or exclude noise injection channels that otherwise may remain poorly understood noise  
581 intrusion paths limiting the sensitivity.  
582

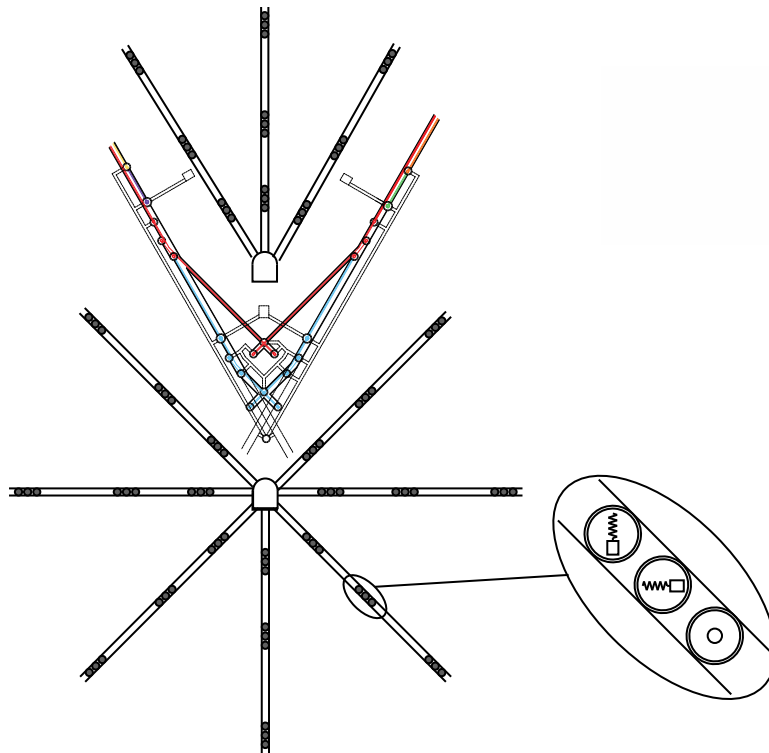


**Figure 7:** Schematic view (not to scale) of radial boreholes and inertial sensor positioning around the corner station for optimal Newtonian noise subtraction. A tunnel in the front and one on the back of the corner station are hypothesized here. The angular density per steradian, the length of the boreholes and the longitudinal positioning of the sensors are chosen to optimize the sensor density for Newtonian noise subtraction while minimizing the borehole length. A crawler positions, levels and aligns the sensors at the desired distance along the borehole, see text for detail.

## 8. Conclusions

The first and foremost gain from the tunnel topology proposed here is the improvement of the observatory astronomical observation efficiency. The physical separation of the test masses, the recombination optics of different detectors and the support point of the isolation chains, as well as the relegation of noisy equipment in separate and sealed excavations will allow continuous astronomical observation mode in most detectors even while work is done on others for staged installation, maintenance, or upgrades. Gaps in gravitational wave observations and the risk of missing a rare, potentially multiple-messenger event like a close-by supernova or a neutron star merger are eliminated.

The second advantage is that arbitrarily long attenuation chains built into the rock environment push the seismic noise farther from the detector noise budget and keep the door open for future sensitivity improvements. Perhaps more importantly, lower frequency attenuation and smaller residual motion reduce the force required for controls and the chance that control noise may end up limiting the detection sensitivity.

The cost of boring and of high-quality inertial sensing instruments is relevant, and the quality of sensors continuously improves. It will take years before the Newtonian noise will represent a limit to sensitivity. Therefore it is probably wise to delay implementation of instruments for full-fledged Newtonian noise subtraction. The proposed tunnel topology is suitable for staging without interrupting astronomical observations.

## Acknowledgments

The authors are grateful to the ET Sardinia host team, to the Istituto Nazionale di Fisica Nucleare (INFN) and the Italian Ministry of the Education, University and Research (MIUR) under the agreement 0021983-06/03/2018, for the borehole seismic data used with the suspension transfer functions studied in this work.

RDS likes to remember the many discussions with his late father Francesco, mining engineer and mine director, he contributed many of the ideas presented in this paper.

The figures representing examples of seismic attenuation components were originally provided by RDS for KAGRA.

We would like to thank Alessandro Bertolini, Aniello Grado, Francesco Fidecaro, Giacomo Oggiano, Joris van Heijningen for useful criticism and discussions and Gianni Gennaro for the KAGRA graphics.

### Appendix (Online Only)

In this section we present

- examples of a typical seismic attenuation chain and illustration of the kind of external support structures that may become necessary if the seismic attenuation chains are not connected directly to hard rock
- an interactive illustration of a tunnel topology satisfying the requirements of the Einstein telescope detectors

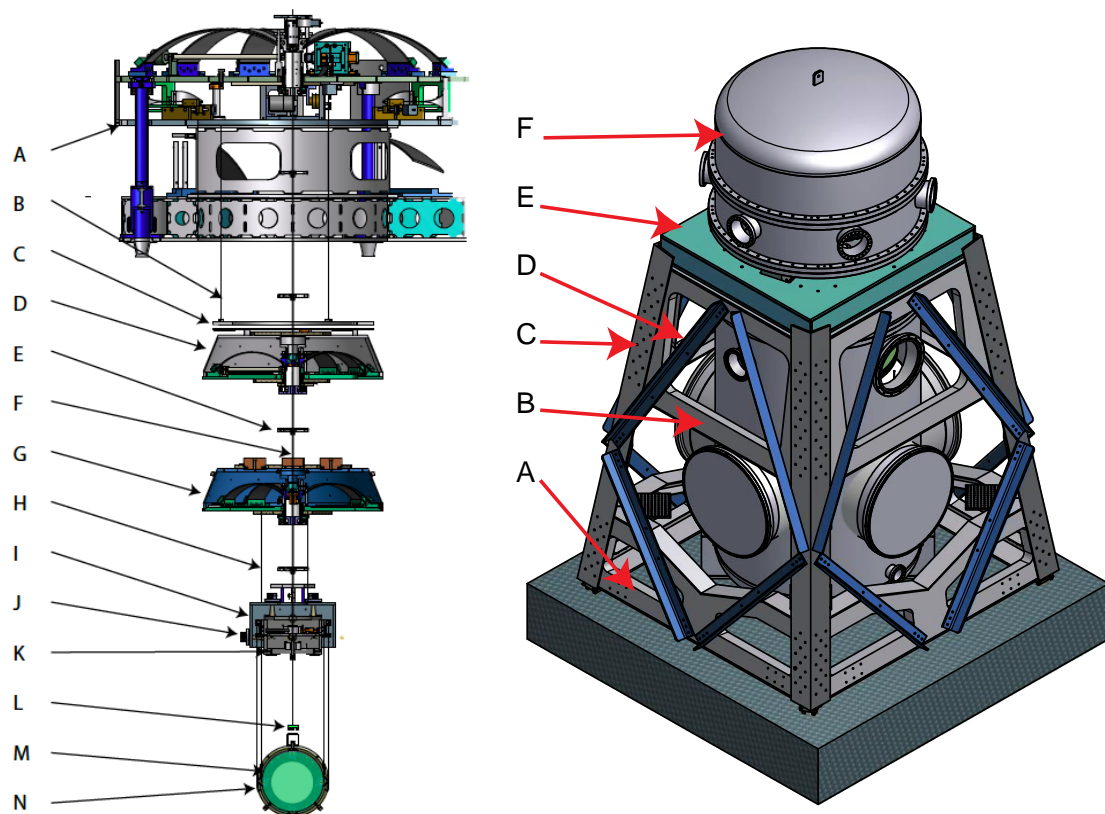
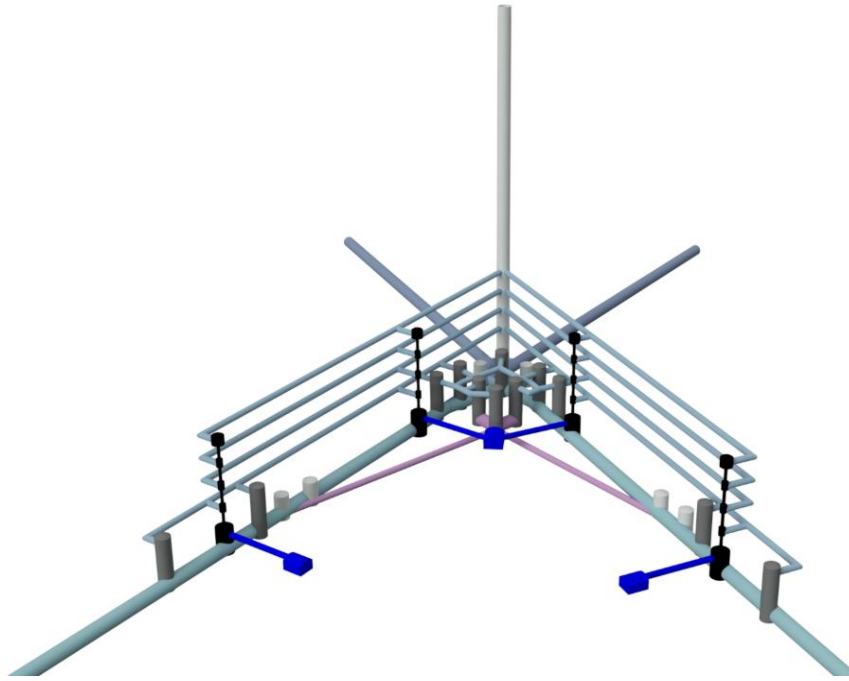


**Figure 8:** Left: Example of a typical seismic attenuation chain; length of wires, size and number of filters would depend on the mass and requirements of the optical payload. A: Pre-Isolator, B: Magnetic damper wires, C: Magnetic damper disk, D: Standard filter, E: cabling spider, F: Suspension wire, G: Bottom filter, H: suspension wires of intermediate mass control box, I: intermediate mass control box, J: OSEM position sensor/actuator, K: Intermediate mass, L: whip magnetic damper of mirror recoil mass, M: mirror, N: mirror recoil mass. Right: Illustration of an external support structure supporting the seismic attenuation head of a compact Seismic attenuation chain. Bolted structures are always found to have resonances different and lower in frequency by as much as a factor of 2 than in simulations. This is because in simulations connections between parts are rigid, as welded, while in bolted structures the connections are always the weakest point. To mitigate this, this support structure is built by two welded frames (A and B) connected by four over-bolted heavy L-beams (C). Over-bolting was common in building bridges before welding was introduced and is important to increase resonant frequencies. Lighter, angled, bolted L-beams (D) sandwiching a



643  
644  
645  
646  
647

dissipative rubber layer both stiffen and damp these resonances. The top platform (E) supports, through bellows, a short, inverted pendulum pre-attenuator like that of figure 5 housed in a removable dome (F). A much larger and more complex structure would be necessary for the test masses to avoid amplifying low frequency seismic tilt noise. Such structures would heavily encumber the space around the test masses.



648  
649

650  
651  
652  
653  
654  
655  
656  
657  
658

**Figure 9:** Interactive illustration of a possible tunnel configuration with access to the different alcoves and raise bore wells housing the components of the gravitational wave detectors (the interactive file can be downloaded from [here](#) and rendered using this [viewer](#)). All noisy components, like the cryogenic chillers, are housed in separate alcoves to confine their noise. The tall vertical well, may extend to the surface providing a required secondary escape route. Note, the main tunnels are illustrated as extending beyond the crossing point. A horizontal tunnel may house the required mode cleaner and vacuum squeezing cavity. The second, angling up, may be the TBM arrival route. If it was convenient to assemble the TBM at the surface the tunnel would provide the main access route.

659

## 660 References

- 661 1. ET Steering Committee Editorial Team. Design Report Update 2020 for the Einstein Telescope. *ET-0007A-20*. **2020**
- 662 2. Accadia, T. et al., The seismic Superattenuators of the Virgo gravitational waves interferometer. *J. Low Freq. Noise Vib. Active Control*, **2010**, *29*, 63 – 79.
- 663 3. Harms, J., Terrestrial gravity fluctuations. *Living Rev. Relativ.*, **2019**, *22*, 6.
- 664 4. Beccaria, M. et al., Relevance of Newtonian seismic noise for the VIRGO interferometer sensitivity. *Class. Quantum Grav.*, **1998**, *15*, 3339.
- 665 5. Creighton, T., Tumbleweeds and airborne gravitational noise sources for LIGO, *Class. Quantum Grav.*, **2008**, *25*, 12.
- 666 6. Brundu, D. et al., Atmospheric Newtonian noise modeling for third-generation gravitational wave detectors. *ArXiv*, **2022**, *arXiv:2206.02610*.
- 667 7. Badaracco, F.; Harms, J., Optimization of seismometer arrays for the cancellation of Newtonian noise from seismic body waves. *Class. Quantum Grav.*, **2019**, *36*, 14.
- 668 8. Abernathy, M. et al., Einstein gravitational wave Telescope conceptual design study, **2011**, ET-0106C-10.
- 669 9. Reitze, D. et al., Cosmic explorer: the US Contribution to gravitational-wave astronomy beyond LIGO. *ArXiv*, **2019**, *arXiv:1907.04833*
- 670 10. Karsten, D.; the LISA study team, LISA: laser interferometer space antenna for gravitational wave measurements. *Class. Quantum Grav.*, **1996**, *13*, A247.

674  
675  
676

- 677 11. Kawamura, S. et al., The Japanese space gravitational wave antenna—DECIGO. *Class. Quantum Grav.*, **2006**, *23*, 8.
- 678 12. Harms, J. et al., Lunar Gravitational-wave Antenna, *Astroph. J.*, **2021**, *910*, 1.
- 679 13. Jani, K.; Loeb, A., Gravitational-wave Lunar Observatory for Cosmology. *J. Cosm. Astropart. Phys.*, **2021**, 044.
- 680 14. Lognonné, P. et al., Lunar Seismic and Gravitational Antenna (LSGA) [Online], **2021**, Available at:  
681 [https://ideas.esa.int/servlet/hype/IMT?documentTableId=45087607031744010&userAction=Browse&templateName=&docu-](https://ideas.esa.int/servlet/hype/IMT?documentTableId=45087607031744010&userAction=Browse&templateName=&documentId=a315450fae481074411ef65e4c5b7746)  
682 [mentId=a315450fae481074411ef65e4c5b7746](https://ideas.esa.int/servlet/hype/IMT?documentTableId=45087607031744010&userAction=Browse&templateName=&documentId=a315450fae481074411ef65e4c5b7746) [Accessed 29 January 2022]
- 683 15. Sathyaprakash B et al., Scientific objectives of Einstein Telescope, **2012**, *Class. Quantum Grav.* *29* 124013
- 684 16. Hild, S. et al., A xylophone configuration for a third-generation gravitational wave detector. *Class. Quantum Grav.*, **2009**, *27*, 1.
- 685 17. Aasi, J. et al., Advanced LIGO, *Class. Quantum Grav.*, **2015**, *32*, 7.
- 686 18. Acernese, F. et al., Advanced Virgo: a second-generation interferometric gravitational wave detector, *Class. Quantum Grav.*,  
687 **2014**, *32*, 2.
- 688 19. Akutsu, T. et al., Construction of KAGRA: an underground gravitational-wave observatory, *Prog. Theo. Exper. Phys.*, **2018**, 1.
- 689 20. Hoek, E., Brown, E. T. & ASCE, M., 1980. Empirical strength criterion for rock masses. *Journal of the geotechnical engineering*  
690 *division*, *106*(9), pp. 1013-1035.
- 691 21. Naticchioni, L. et al., Characterization of the Sos Enattos site for the Einstein Telescope, *J. of Phys.: Conf. Series*, **2020**, *1468*, 012242.
- 692 22. DeSalvo, R.; Blow, J.; Pineda Bosque, C.; Selleri, S., Angled beam expander telescopes for the Michelson beams in third genera-  
693 *tion gravitational wave observatories*, *Class. Quantum Grav.*, **2022**, *39*, 4.
- 694 23. Harms, J. et al., Characterization of the seismic environment at the Sanford Underground Laboratory, South Dakota. *Class.*  
695 *Quantum Grav.*, **2010**, *27*, 22.
- 696 24. Wannemacher, M. H., Private communication, **2020**, Austria: Implenia.
- 697 25. Saulson, P. R., Seismic Noise and Vibration Isolation. In: *Fundamentals of interferometric gravitational wave detectors*, World  
698 *Scientific*, **1994**, pp. 127-142.
- 699 26. Buikema, A. et al, Sensitivity and performance of the Advanced LIGO detectors in the third observing run, *Phys. Rev. D*, **2020**,  
700 *102*, 062003.
- 701 27. Singh Ubhi, A. et al., Active platform stabilization with a 6D seismometer, **2022**, arXiv:2207.10417
- 702 28. Cella, G. et al., Seismic attenuation performance of the first prototype of a geometric anti-spring filter. *Nucl. Instrum.*, **2002**, *487*,  
703 *652-660*.
- 704 29. Cella, G. et al., Monolithic geometric anti-spring blades. *Nucl. Instrum.*, **2005**, *540*, 502-519.
- 705 30. ORFEUS, Observatories & Research Facilities for European Seismology [Online], **2022**, Available at: <http://orfeus-eu.org/> [Ac-  
706 *cessed 3 January 2022*].
- 707 31. Chen, D. et al., Vibration measurement in the KAGRA cryostat, *Class. Quantum Grav.*, **2014**, *31*, 22.
- 708 32. Ando M, TAMA collaboration. Current status of the TAMA300 gravitational-wave detector. *Classical and Quantum Gravity*. **2005**  
709 *Aug 23;22*(18): S881
- 710 33. Aso Y, Michimura Y, Somiya K, Ando M, Miyakawa O, Sekiguchi T, Tatsumi D, Yamamoto H, Kagra Collaboration. Interfer-  
711 *ometer design of the KAGRA gravitational wave detector*. *Physical Review D*. **2013 Aug 20;88**(4):043007.
- 712 34. L Busch and S Grohmann. Conceptual layout of a helium cooling system for the Einstein Telescope. *IOP Conf. Ser.: Mater. Sci.*  
713 *Eng*, **2022**, *1240* 012095
- 714 35. Van Heijningen, J. V., Bertolini, A., Hennes, E., Beker, M. G., Doets, M., Bulten, H. J., ... & Van den Brand, J. F. J. A multistage  
715 *vibration isolation system for Advanced Virgo suspended optical benches*. *Classical and Quantum Gravity*, **2019**, *36*(7), 075007.
- 716 36. Sannibale, V. et al., Recent results of a seismically isolated optical table prototype designed for advanced LIGO, *J. of Phys.: Conf.*  
717 *Series*, **2008**, *122*, 1.
- 718 37. Marka, S. et al., Anatomy of the TAMA SAS seismic attenuation system, *Class. Quantum Grav.*, **2002**, *19*, 7.
- 719 38. DeSalvo, R., Passive, nonlinear, mechanical structures for seismic attenuation. *J. Comput. Nonlinear Dyn.*, **2007**, *2*, 290-298.
- 720 39. Virdone, N. et al., Extended-time-scale creep measurement on Maraging cantilever blade springs, *Nucl. Instrum.*, **2008**, *593*, 597-  
721 *607*.
- 722 40. Takamori, A. et al., Inverted pendulum as low-frequency pre-isolation for advanced gravitational wave detectors, *Nucl. In-*  
723 *strument.*, **2007**, *582*, 683-92.
- 724 41. Tshilumba, D. et al, Vibration analysis and control of the LIGO observatories large chambers and support piers. *ISMA2014 Proc.*,  
725 **2014**, 187-200.
- 726 42. Accadia, T. et al., A state observer for the Virgo inverted pendulum. *Rev. Sci. Instrum.*, **2011**, *82*, 094502.
- 727 43. Stochino, A. et al., The Seismic Attenuation System (SAS) for the Advanced LIGO gravitational wave interferometric detectors,  
728 *Nucl. Instrum.*, **2009**, *598*, 737-753.
- 729 44. Losurdo, G. et al., An inverted pendulum preisolator stage for the VIRGO suspension system, *Rev. Sci. Instrum.*, **1999**, *70*, 2507-  
730 *2515*.
- 731 45. Hua, W. et al., Low-frequency active vibration isolation for advanced LIGO, *Grav. Wave Part. Astrophys. Det.*, **2004**, *5500*, 194-205.
- 732 46. Wanner, A. et al, Seismic attenuation system for the AEI 10 meter Prototype, *Class. Quantum Grav.*, **2012**, *29*, 24.
- 733 47. Dahl, K. et al., Suspension platform interferometer for the AEI 10 m prototype: concept, design and optical layout, *Class. Quan-*  
734 *tum Grav.*, **2012**, *29*, 9.
- 735 48. Kirchoff, R. et al., Local active isolation of the AEI-SAS for the AEI 10 m prototype facility, *Class. Quantum Grav.*, **2020**, *37*, 11.
- 736 49. Marvin, A.; Lantz, B., Enhanced Feed-Forward Control for Advanced LIGO, **2013**, LIGO Document T1300907-v1.

- 737 50. Cumming, A. V. et al., Proposed large scale monolithic fused silica mirror suspension for 3rd generation gravitational wave  
738 detectors, *ArXiv*. **2021**, arXiv:2111.09119.
- 739 51. Amico, P. et al., Thermal noise reduction for present and future gravitational wave detectors. *Nucl. Instrum.*, **2004**, *518*, pp. 240-  
740 243.
- 741 52. Khalaidovski, A. H. G. C. D. et al., Evaluation of heat extraction through sapphire fibers for the GW observatory KAGRA, *Class.*  
742 *Quantum Grav.*, **2014**, *31*, 10.
- 743 53. Badaracco, F. et al., A new approach for suspending cryogenic mirrors, **2022**, ET Docs, ET-0060A-22.
- 744 54. Milazzo, E., Private communication, **2020**, Caltanissetta, Italy: S&C S.r.l. Servizi e Consulenze.

745

746

747

748

749

750

751

752

753

754